Analyst

COMMUNICATION

Enzymatic conversion of magnetic nanoparticles to a non-magnetic precipitate: a new approach to magnetic sensing

Arati G. Kolhatkar,[a] Andrew C. Jamison,[a] Ivan Nekrashevich,[b] Katerina Kourentzi,[c] Dmitri Litvinov,*[a,b] Audrius Brazdeikis,*[d] Richard C. Willson*[c,e,f] and T. Randall Lee*[a]

Cite this: *Analyst*, 2016, **141**, 5246

Received 25th March 2016,
Accepted 24th July 2016

DOI: 10.1039/c6an00709k

www.rsc.org/analyst

Magnetic sensing utilizes the detection of biomolecule-conjugated magnetic nanoparticles (MNPs). Our new strategy offers a novel approach to magnetic sensing where *in situ* conversion produces a "loss of signal" in the sensing device. This report demonstrates the enzymatic conversion of Fe_3O_4 MNPs to a non-magnetic precipitate *via* reduction by L-ascorbic acid generated by the action of alkaline phosphatase.

Magnetic nanoparticles (MNPs) are commonly used in off-line sample capture, clean-up, and concentration, and as labels for sensitive biomolecule detection.[1] In contrast to optical labels, magnetic labels eliminate concerns regarding photobleaching and can be potentially more sensitive, even in the presence of turbidity, due to the absence of magnetic background in biological samples. Recent advances in sensor technology have made possible the high-sensitivity detection of MNP samples using giant magnetoresistive (GMR) sensors. The application of these sensors in biomolecular recognition was pioneered by Baselt *et al.* in 1998,[2] and then demonstrated by Shieh and Ackley in 2000.[3] In the classical approach to magnetic biosensing, magnetic particles are functionalized, attached to biomarkers, and then detected by a change in resistance in the layered magnetoresistive element of the GMR sensor. There are several research groups that have advanced magnetic sensor technologies at the micrometer scale.[4] Commercially produced magnetic immunoassays include MagArray (GMR-based – utilizing 50 nm magnetic nanotags),[5] MagniSense (reader that registers a nonlinear particle magnetization signature – utilizing 50 nm paramagnetic particles),[6] and MagnaBiosciences (lateral flow assays – utilizing 60–380 nm paramagnetic particles).[7] Our assay utilizes a vibrating sample magnetometer (VSM), an AC susceptometer, and ultimately a custom-built GMR sensor.

This report introduces a new approach to magnetic sensing based on the enzymatic modification of MNP tags through the generation of an intermediate reducing agent. Conventional enzyme-linked immunosorbent assays (ELISA) using alkaline phosphatase (AP) as the reporter rely on the dephosphorylation of a substrate such as 4-nitrophenyl phosphate, 4-methylumbelliferyl phosphate (4-MUP), or 3-(2′-spiroadaman-tane)-4-methoxy-4-(3′-phosphoryl-oxy)phenyl-1,2-dioxetane (AMPPD, in the form of a disodium salt), to form a product that can be detected by its absorbance, fluorescence, or luminescence (Fig. 1). In cases where an insoluble colored product is required for detection, bromochloroindolyl phosphate-nitroblue tetrazolium (BCIP-NBT), which forms a blue precipitate/chromophore upon dephosphorylation, can be used as a substrate.[8] An alternative approach to a visual result would be the widely-used silver enhancement or "silver staining" technique, where AP is employed to produce metallic silver by reduction of silver ions utilizing a reducing agent that is only formed after the AP-catalyzed dephosphorylation of a substrate (*e.g.*, phosphorylated L-ascorbic acid,[9] 4-aminophenyl phosphate,[10] or 3-indoxyl phosphate).[11] Additionally, there have been a number of recent reports that have focused on

[a]*Department of Chemistry and Texas Center for Superconductivity, University of Houston, 4800 Calhoun Road, Houston, TX 77204, USA. E-mail: litvinov@uh.edu, trlee@uh.edu*
[b]*Department of Electrical and Computer Engineering, University of Houston, 4800 Calhoun Road, Houston, TX 77204, USA*
[c]*Department of Chemical and Biomolecular Engineering, University of Houston, 4726 Calhoun Road, Houston, TX 77204, USA*
[d]*Department of Physics and Texas Center for Superconductivity, University of Houston, 4800 Calhoun Road, Houston, TX 77204, USA. E-mail: audrius@uh.edu*
[e]*Department of Biology and Biochemistry, University of Houston, 4800 Calhoun Road, Houston, TX 77204, USA. E-mail: willson@uh.edu*
[f]*Instituto Tecnológico de Monterrey, Monterrey, Mexico*

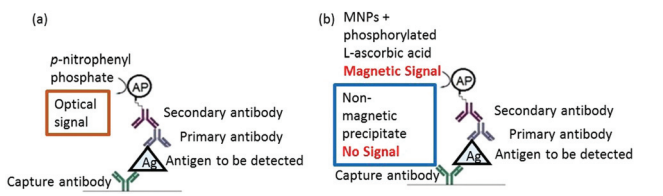

Fig. 1 Schematic of (a) conventional ELISA – detection by optical signal and (b) our strategy – detection by loss of magnetic signal. Figure adapted from ref. 21 and 22.

"biometallization" – the electrochemical deposition of a metal in the presence of an enzyme.[12,13]

Here we propose that the disappearance of MNPs, and thus a loss of signal, also can provide a convenient and sensitive method for detection of AP as a label (Fig. 1) or for detection of AP itself (Fig. 2). AP plays an important role in cell cycle, growth, and apoptosis, and research efforts continue to study detection of serum AP as a biomarker.[14] Some conditions, such as rapid bone growth (during puberty), bone disease (Paget's disease or cancer that has spread to the bones), hyperparathyroidism, vitamin D deficiency, or damaged liver cells, result in high blood AP levels. While the detection of AP using fluorescence[15–17] and electrochemical[18,19] assays has been studied (Table 1), this report provides the first proof-of-concept of a magnetic assay.

In addition to enzyme-mediated silver staining, L-ascorbic acid has also been used directly, without enzymatic conversion from phosphorylated L-ascorbic acid, to reduce salts such as $AgNO_3$, $HAuCl_4$, Pt, Pd, $CuSO_4$, $Co(NO_3)_2$, $Fe(NO_3)_2$, and $MoCl_2$ to yield nanoparticles of Ag, Au, Pt, Pd, Cu, Co_3O_4, Fe_2O_3, and MoO_2, respectively.[13,22,23] However, other than the enzymatically synthesized magnetic nanoparticles by Kolhatkar *et al.*[22] these reports make no mention of the development of magnetic products. Also, during the synthesis of Fe_3O_4 nanoparticles *via* the reduction of ferric chloride by L-ascorbic acid, Lv *et al.*[24] serendipitously observed that an excess of L-ascorbic acid failed to generate Fe_3O_4 MNPs because the excess L-ascorbic acid likely reduced the Fe^{3+} in the synthesized-Fe_3O_4 as well.[20] The fate of the elemental components in this effort to produce MNPs does point to the possible development of a system where the magnetic component loses its magnetism through a reduction process.

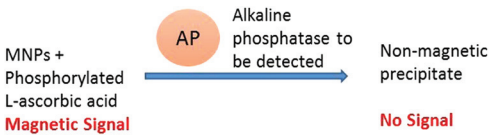

Fig. 2 Detection of AP by loss of magnetic signal.

Table 1 Detection limits of AP for different assays

Method	Detection limit
Optical ELISA absorbance at 450 nm	2.0 U L^{-1}
Fluorescence assay using quantum dots[15]	1.4 U L^{-1}
Electrochemical assay[19]	0.1 U L^{-1}
Fluorescence assay using resorufin; simultaneous AP detection and cell imaging[20]	0.1 U L^{-1}
Fluorescence assay using quantum dots[16]	1.1 U L^{-1}
Our magnetic assay – loss of signal	
(i) AC susceptometer	0.5 kU L^{-1}
(ii) VSM	0.01 U L^{-1}
(iii) GMR sensor (theoretical limit based on GMR sensitivity of 10^{-13} emu)	pU L^{-1}

Because of the implications in terms of iron availability and cycling, parallel research to study the fate of iron oxides in the environment is ongoing, yielding useful background for this report. Nanoscale iron oxides (*e.g.*, ferrihydrite, hematite, goethite) are ubiquitous in nature, and their fate in the environment arises from their chemical reactivity. Several studies used ascorbic acid as a model compound to study the reductive dissolution of nanoparticles prepared from the aforementioned minerals.[15,19,20] In all cases (varying size, pH, morphology), insoluble salts incorporating Fe^{3+} were reduced to soluble salts of Fe^{2+} in the presence of ascorbic acid. We wished to confirm the ability of L-ascorbic acid to reduce presynthesized Fe_3O_4 MNPs, both using L-ascorbic acid purchased from a chemical supplier and using L-ascorbic acid enzymatically formed *in situ* to determine the fate of their magnetic properties. For our enzymatic reduction, AP catalyzed the dephosphorylation of L-ascorbic-2-phosphate to L-ascorbic acid, which then served as a reducing agent for the Fe_3O_4 MNPs.

This manuscript reports the first use of an enzyme to convert MNPs to a non-magnetic precipitate, with the aim of changing/reducing the resistance that is registered using a GMR sensor – a potentially elegant approach that should prove useful in biosensing using AP as a label (Fig. 1) or for detecting AP itself (Fig. 2). For the preparation of our MNPs, we modified the procedure reported by Deng *et al.*[25] to obtain spherical Fe_3O_4 nanoparticles having diameters of 100 nm. This synthesis involved sequentially dissolving iron chloride (1.4 g, $FeCl_3{\cdot}6H_2O$) and sodium acetate (3.6 g) in 15 mL of ethylene glycol. The solution was stirred for an additional 30 min and then injected at once into a round-bottomed flask containing a vigorously stirred solution of PVP (0.40 g) in 35 mL of ethylene glycol heated to and kept at 180 °C. The mixture was then vigorously stirred for 6 h during which a black precipitate was obtained, washed multiple times with ethanol and purified water, and dried under vacuum at room temperature.

The ascorbic acid (aa) used in these experiments was either a purchased chemical ("chemical synthesis" approach) or an enzymatically produced chemical formed *via* dephosphorylation of L-ascorbic acid 2-phosphate sesquimagnesium salt hydrate (p-aa) by alkaline phosphatase (AP) ("enzymatic synthesis" approach). Samples of AP were obtained from Sigma (catalog # P6774; 0.049 mL; 3531 units per mg protein and 13 mg protein per mL for all experiments except those using the AC susceptometer and catalog # P6774; 0.046 mL; 2703 units per mg protein and 16 mg protein per mL for experiments involving the AC susceptometer). One activity unit of AP is defined to hydrolyze 1 μmol of substrate (4-nitrophenyl phosphate) per minute at pH 9.8 at 37 °C. Zeba desalting columns (7K MWCO from Thermo Fisher Scientific) were used to remove more than 95% (column specification) of the salts (5 mM $MgCl_2$ and 0.2 mM $ZnCl_2$) present in the AP solution. The enzyme was then resuspended in 1000 μL diethanolamine buffer (pH 9.8) containing 5 mM $MgNO_3$ and 0.25 mM $ZnNO_3$ to give a final concentration of about 2 units

AP per μL. In a 50 mL centrifuge tube, 0.25 mL of 1 mg mL^{-1} 100 nm Fe_3O_4 MNPs was added to 5 mL of purified water. For chemical or enzymatic conversion, 0.05 and 0.1 g (0.3 and 0.6 mmol) of aa or 0.1 g (0.3 mmol) of p-aa, respectively, were added to the solution. In the case of enzymatic conversion, 5 μL of 2 units per μL AP enzyme was added to the centrifuge tube containing the MNPs and p-aa. The experiment was carried out at 20 °C (room temperature). The chemicals used in the syntheses were of analytical grade and were used as received from the suppliers without further purification. Purified water (resistivity of >18 MΩ cm) from a Milli-Q water system was used in the synthesis and washing steps. To evaluate the *in situ* kinetics of loss of magnetization, we added 2 to 20 μL of ~2 units per μL AP enzyme to 0.15 mL of 0.33 to 1.0 mg mL^{-1} MNPs and 0.15 mL of 0.1 g mL^{-1} p-aa and monitored changes in the apparent magnetization using AC susceptometry.

The MNPs and the resulting non-magnetic precipitate were characterized by scanning electron microscopy (SEM; LEO-1525 operating at 15 kV and equipped with an energy-dispersive X-ray spectrometer, EDX), vibrating sample magnetometry (VSM; LakeShore, Model VSM 7300 Series with a LakeShore Model 735 Controller and LakeShore Model 450 Gmeter Software, Version 3.8.0), and X-ray diffractometry (XRD; Siemens D5000 X-ray diffractometer). For the SEM analyses, we deposited the MNPs or non-magnetic precipitate on a silicon wafer and allowed the samples to dry. We used EDX and XRD to confirm the composition of the samples. For the XRD studies, a concentrated sample of nanoparticles in ethanol was deposited on a piranha-cleaned glass slide, and XRD was carried out using Cu Kα radiation (λ = 1.540562 Å) in the 2θ range from 0 to 90°. The magnetic properties (saturation magnetization, residual magnetization, coercivity, and blocking temperature) of a known mass of sample were measured using VSM. Saturation magnetization and coercivity were obtained from the hysteresis loop for data collected at 300 K. In addition to end-point measurements in the static field using VSM, we recorded a time profile of loss of magnetization using an AC susceptometer. The AC magnetic susceptibility was measured at 10 kHz in a zero-bias DC field using two physically separated primary/secondary coil pairs. The sample response (vector voltage) was measured by a differential pre-amplifier and a digital phase sensitive detector yielding a complex magnetic susceptibility. A compensating vector voltage phase-lock to the primary drive current was always applied to assure that each sample was measured with maximum sensitivity.

Prior to testing the enzymatic conversion of MNPs to a non-magnetic precipitate, we used purchased L-ascorbic acid to evaluate its efficiency for reducing Fe_3O_4 MNPs. In the presence of both 3 and 6 mmol L-ascorbic acid, the black-brown-colored Fe_3O_4 MNP solution (0.25 mL of 0.001 g mL^{-1} Fe_3O_4 MNPs suspended in 5 mL of purified water) became completely clear in about 2 h. In the enzymatic process, the solution did not become clear, and a white precipitate was observed in about 5 h. The white precipitate was characterized utilizing the various methods used for characterization of the MNPs (described earlier). The SEM images of the Fe_3O_4 MNPs and the product of the enzymatic conversion are shown in Fig. 3. When the chemical L-ascorbic acid was used as purchased for the MNP reduction, Fe^{3+} was reduced to a soluble salt of Fe^{2+}, yielding a particle decomposition with no precipitate; therefore, we have no images to report for the chemically-converted Fe_3O_4 MNPs.

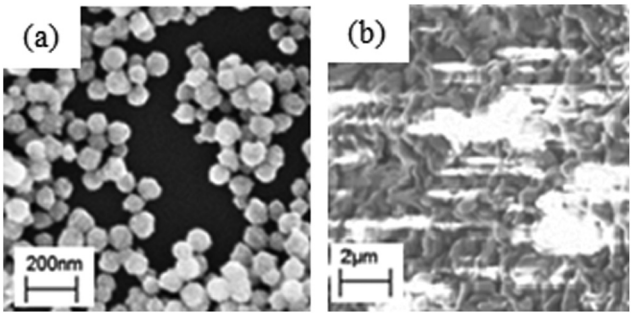

Fig. 3 SEM images of (a) 100 nm Fe_3O_4 MNPs and (b) the non-magnetic precipitate obtained from the enzymatic conversion of the 100 nm Fe_3O_4 MNPs.

Regarding the formation of the white precipitate, there has been significant research on the mechanism of alkaline phosphatase dephosphorylation.[26] To evaluate the role of phosphate, we examined three experimental conditions with MNPs in deionized water (no enzyme): (1) with ascorbic acid, (2) with ascorbic acid + potassium phosphate but without pH adjustment, and (3) with ascorbic acid + potassium phosphate adjusted to pH 9 (optimum pH for alkaline phosphatase). As a control, we used the MNPs in deionized water alone. Conditions (1) and (2) yielded a clear solution, and condition (3), which included phosphate at alkaline pH, led to the formation of a precipitate. The control showed that the MNPs were stable in water. These results are consistent with a model in which phosphate under alkaline conditions is responsible for the difference in the observed results (white precipitate *versus* total dissolution, respectively).

When contemplating our results, we investigated other possible contributions to the loss of magnetization. It has been documented that AP has a high turnover number for various phosphorylated substrates.[27] In our experiment, there are no competing substrates and demonstrating selectivity of the enzyme towards L-ascorbic acid 2-phosphate sesquimagnesium salt hydrate is not required. The Fe_3O_4 MNPs used in the experiment are stable way beyond the duration of the experiment[28] and, similarly, the AP enzyme is stable under the chosen pH and temperature conditions.[29]

Fig. 4 shows the elemental composition of the non-magnetic precipitate obtained from the enzymatic procedure as measured by SEM/EDX. The SEM/EDX spectrum represents the average of data collected for 5 samples. The EDX data show that the composition of the non-magnetic precipitate obtained from the enzymatic conversion of the 100 nm Fe_3O_4 MNPs is $Fe_{27\pm5}O_{73\pm5}$.

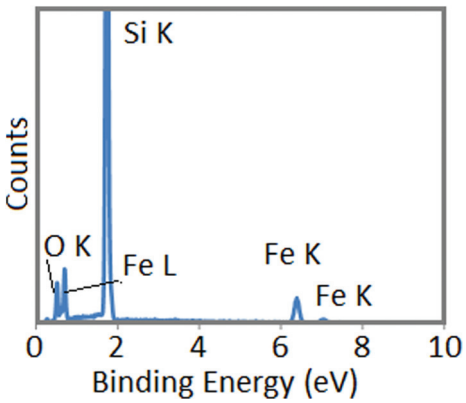

Fig. 4 Composition of enzymatically-formed non-magnetic precipitate determined by SEM-EDX.

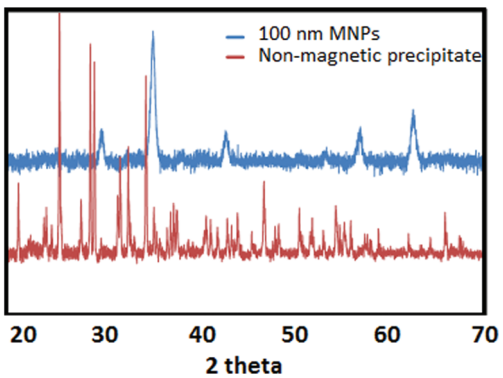

Fig. 5 Comparison of the XRD pattern of the non-magnetic precipitate obtained by enzymatic reduction of the 100 nm Fe_3O_4 MNPs *versus* that of the 100 nm Fe_3O_4 MNPs.

Fig. 5 compares the XRD patterns of the Fe_3O_4 MNPs and the enzymatically-synthesized non-magnetic precipitate. The MNP XRD pattern confirms that the MNP samples are Fe_3O_4 since the pattern matches that of Fe_3O_4 in the Inorganic Crystal Structure Database (ICSD Collection Code 26410). We characterized the non-magnetic precipitate using XRD and compared its pattern to that of the Fe_3O_4 MNPs, as shown in Fig. 5. Comparison of the XRD patterns confirms that the non-magnetic precipitate is distinctly different from the original Fe_3O_4 MNPs.

We also calculated elemental compositions and mass balances for the conversion process. Based on the experimental protocol described above, 27 μg of 0.9 units of AP protein (Sigma, catalog # P6774: 0.049 mL containing 13 mg protein per mL and 3531 units per mg protein) dephosphorylated phosphorylated L-ascorbic acid to yield L-ascorbic acid that reduced 100 nm Fe_3O_4 MNPs (weight% ratio of Fe : O of 72 : 28) to obtain 0.0005 g non-magnetic $Fe_{27\pm5}O_{73\pm5}$ with a weight% ratio Fe : O of 56 ± 5 : 44 ± 5.

Fig. 6 shows the magnetic properties of the Fe_3O_4 MNPs obtained by analysis using VSM. The saturation magnetization and coercivity of the 100 nm Fe_3O_4 MNPs were 70 emu g^{-1} and 23 G, respectively. Fig. 6 also shows that after the MNPs were enzymatically reduced, the precipitate exhibited no measurable saturation magnetization at room temperature. In separate studies, we also found that, unlike the Fe_3O_4 MNPs, the enzymatic precipitate showed no attraction to a bar magnet.

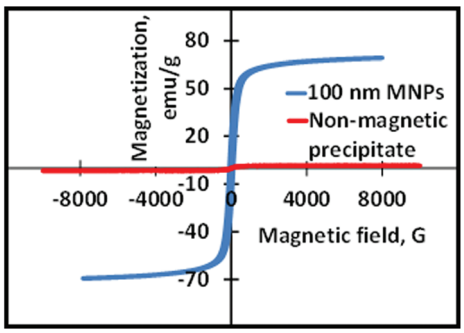

Fig. 6 Magnetization curves recorded at 300 K for the 100 nm Fe_3O_4 MNPs.

Fig. 7 highlights the *in situ* conversion of MNPs to a non-magnetic precipitate using AC susceptometry, which monitored the loss of magnetization with time. As described earlier, chemical reduction of MNPs yielded a clear solution and a loss in magnetization in less than 2 hours. Enzymatic conversion of MNPs to a non-magnetic precipitate (as characterized using VSM and shown in Fig. 6) took 5 h. However, the drop in magnetization in the enzymatic experiment took about 96 hours. Loss of magnetization was observed using 2 and 20 μL of ~2 units per μL AP enzyme to convert 0.33 mg mL^{-1} concentration of 100 nm MNPs. Both demonstrated loss in magnetization in the same time period. Although there is room for improvement for its use in diagnostics, Fig. 7 clearly demonstrates

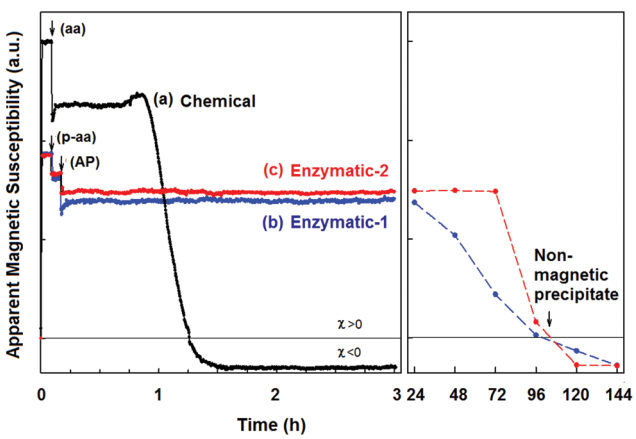

Fig. 7 Loss of magnetization monitored by AC susceptometry (a) chemical: aa – ascorbic acid (black line), (b) enzymatic: 20 μL of 2 U mL^{-1} AP (blue line), and (c) enzymatic: 2 μL of 2 U mL^{-1} AP (red line). Both (b) and (c) used phosphorylated ascorbic acid (p-aa) and alkaline phosphatase enzyme (AP).

proof-of-concept that this procedure can be used as a "loss of signal" method for ELISA or for detection of AP itself. The experiment involves dephosphorylation of phosphorylated ascorbic acid (to ascorbic acid) catalyzed by the biomarker (enzyme) that is specific only toward phosphorylated substrates. Subsequent reduction of MNPs by this *in situ*-produced ascorbic acid then leads to a non-magnetic precipitate. Regarding possible competing reducing agents, ascorbic acid and glutathione (GSH) are the most commonly found reducing agents in living tissue.[30] However, the interaction of glutathione (GSH) with ascorbic acid and the redox reactions between GSH/GSSG (oxidized GSH) and L-ascorbic/dehydroascorbic acid have been studied in depth, and it has been demonstrated that GSH prevents the *in vitro* oxidation of ascorbic acid.[31] Based on the standard reduction potentials, ascorbic acid (0.06 V) is a better reducing agent than GSH (0.23 V), which in turn *via* redox coupling ensures the regeneration of ascorbic acid. Given these collective considerations, if the detection proceeds *via* ELISA, our new strategy can, in principle, be used to detect any analyte for which AP is used as a label (see Fig. 1).

Our carboxylic acid functionalized model-sensor platform of 400 nm × 400 nm can electrostatically bind to 16 amine-functionalized Fe_3O_4 MNPs having a diameter of 100 nm.[32,33] The conversion of MNPs to non-magnetic precipitate can be monitored using this giant magnetoresistive sensor (GMR) which is designed to detect one Fe_3O_4 MNP possessing a saturation magnetization of 70 emu g^{-1}.[2,32] For detection of AP biomarker, the "loss of signal" method combined with the ultrasensitivity (10^{-13} emu) of the GMR sensor can yield a theoretical detection level of pU L^{-1}. Due to the challenges faced by the GMR production team, we evaluated the effectiveness of the two routes toward the reduction of MNPs using an AC susceptometer based on its portability and sensitivity of less than 10^{-4} emu.[34] With the AC susceptometer, we were able to document a loss of magnetization of 3×10^{13} MNPs with 2 μL of 2 U μL^{-1} AP enzyme in 72 to 96 h. Each experiment with the AC susceptometer was repeated three times, and the non-averaged signal-to noise ratio (SNR) was better than 110 for each measurement shown in Fig. 7, where the SNR is defined as the ratio between the variance of the signal and the variance of the noise measured at the beginning of each experiment.

Using the VSM, we documented a loss of magnetization of 5.5×10^{13} MNPs using 5 μL of 2 U μL^{-1} AP enzyme in 5 h. Although not generally employed as a sensor, the VSM measurements provided us with a sensitivity of 0.01 U L^{-1} for the detection of AP. Each of the methods used has its own sensitivity and sample state (in solution or solid): AC magnetometer (10^{-4} emu or SNR signal-to-noise ratio of 10; liquid; time profile data), VSM (10^{-6} emu; solid; end product characterization), and GMR (10^{-13} emu; solid; end product characterization). Based on the MNP mass required to obtain a measurement and the amount and concentration of AP used for that mass, we determined the detection limits in Table 1 for our magnetic assays.

Conclusions

The strategy outlined in this report offers a novel approach to magnetic sensing. Dephosphorylation of phosphorylated L-ascorbic acid by AP yields L-ascorbic acid, which converts magnetic Fe_3O_4 MNPs to a non-magnetic product. This *in situ* conversion in the course of the assay provides a "loss of signal" option in magnetic sensing applications.

Acknowledgements

We thank the National Science Foundation (ECCS-0926027), the Robert A. Welch Foundation (Grant No. E-1320 to T. R. L. and E-1264 to R. C. W.), CPRIT (Grant RP150343 to R. C. W. and D. L.), the donors of the Huffington-Woestemeyer chair, and the Texas Center for Superconductivity at the University of Houston for generous support.

Notes and references

1 V. Mani and B. V. Chikkaveeraiah, *Expert Opin. Med. Diagn.*, 2011, **5**, 381–391.

2 D. R. Baselt, G. U. Lee, M. Natesan, S. W. Metzger, P. E. Sheehan and R. J. Colton, *Biosens. Bioelectron.*, 1998, **13**, 731–739.

3 R. Shieh and D. E. Ackley, Magnetoresistance-based method and apparatus for molecular detection, *US Pat.*, 6057167A, 2000.

4 Y. Li, B. Srinivasan, Y. Jing, X. Yao, M. A. Hugger, J. P. Wang and C. Xing, *J. Am. Chem. Soc.*, 2010, **132**, 4388–4392; B. Srinivasan, Y. Li, Y. Jing, Y.-H. Xu, X. Yao, C. Xing and J.-P. Wang, *Angew. Chem., Int. Ed.*, 2009, **48**, 2764–2767; B. Srinivasan, Y. Li, Y. Jing, C. Xing, J. Slaton and J.-P. Wang, *Anal. Chem.*, 2011, **83**, 2996–3002; D. A. Hall, R. S. Gaster, T. Lin, S. J. Osterfeld, S. Han, B. Murmann and S. X. Wang, *Biosens. Bioelectron.*, 2010, **25**, 2051–2057; S. J. Osterfeld, H. Yu, R. S. Gaster, S. Caramuta, L. Xu, S. J. Han, D. A. Hall, R. J. Wilson, S. Sun, R. L. White, R. W. Davis, N. Pourmand and S. X. Wang, *Proc. Natl. Acad. Sci. U. S. A.*, 2008, **105**, 20637–20640; D. A. Hall, S. X. Wang, B. Murmann and R. S. Gaster, Conf. Proc. (Midwest Symp. Circuits Syst.), 2010, 1779–1782; R. S. Gaster, D. A. Hall, C. H. Nielsen, S. J. Osterfeld, H. Yu, K. E. Mach, R. J. Wilson, B. Murmann, J. C. Liao, S. S. Gambhir and S. X. Wang, *Nat. Med.*, 2009, **15**, 1327–1332; A. V. Orlov, V. A. Bragina, M. P. Nikitin and P. I. Nikitin, *Biosens. Bioelectron.*, 2016, **79**, 423–429.

5 I. Fenoglio, E. Aldieri, E. Gazzano, F. Cesano, M. Colonna, D. Scarano, G. Mazzucco, A. Attanasio, Y. Yakoub, D. Lison and B. Fibini, *Chem. Res. Toxicol.*, 2012, **25**, 74–82.

6 A. V. Orlov, J. A. Khodakova, M. P. Nikitin, A. O. Shepelyakovskaya, F. A. Brovko, A. G. Laman, E. V. Grishin and P. I. Nikitin, *Anal. Chem.*, 2013, **85**, 1154–1163.

7 R. T. La Borde, R. N. Taff and D. M. Pratt, A lateral flow assay device with improved detection access for immunoassay use, *WIPO*, WO011942A1, 2004; Q. F. Xu, H. Xu, H. Gu, J. B. Li, Y. Wang and M. Wei, *Mater. Sci. Eng., C*, 2009, **29**, 702–707.

8 M. J. Eadie, J. H. Tyrer, J. R. Kukums and W. D. Hooper, *Histochemistry*, 1970, **21**, 170–180; F. P. Altman, *Histochemistry*, 1974, **38**, 155–171.

9 E. E. Cacao, *PhD Dissertation*, University of Houston, Houston, TX, USA, 2012.

10 J. Wu, K. Y. Chumbimuni-Torres, M. Galik, C. Thammakhet, D. A. Haake and J. Wang, *Anal. Chem.*, 2009, **81**, 10007–10012.

11 P. Fanjul-Bolado, D. Hernandez-Santos, M. B. Gonzalez-Garcia and A. Costa-Garcia, *Anal. Chem.*, 2007, **79**, 5272–5277.

12 S. Hwang, E. Kim and J. Kwak, *Anal. Chem.*, 2005, **77**, 579–584; C.-H. Zhou, Z. Wu, J.-J. Chen, C. Xiong, Z. Chen, D.-W. Pang and Z.-L. Zhang, *Chem. – Asian J.*, 2015, **10**, 1387–1393.

13 B. A. Zaccheo and R. M. Crooks, *Anal. Chem.*, 2009, **81**, 5757–5761.

14 N. Badgu and R. Merugu, *Int. J. Res. Pharm. Sci.*, 2013, **4**, 371–379; U. Domar, K. Hirano and T. Stigbrand, *Clin. Chim. Acta*, 1991, **203**, 305–313; H. Harris, *Clin. Chim. Acta*, 1990, **186**, 133–150; M. A. Volodin, I. V. Bokhman, E. G. Shvarev, N. R. Safrannikova and L. A. Kostina, *Akush. Ginekol.*, 1986, 29–31.

15 Z. Qian, L. Chai, C. Tang, Y. Huang, J. Chen and H. Feng, *Anal. Chem.*, 2015, **87**, 2966–2973.

16 Z. S. Qian, L. J. Chai, Y. Y. Huang, C. Tang, J. S. Jia, J. R. Chen and H. Feng, *Biosens. Bioelectron.*, 2015, **68**, 675–680.

17 J. Deng, P. Yu, Y. Wang and L. Mao, *Anal. Chem.*, 2015, **87**, 3080–3086.

18 S. Goggins, C. Naz, B. J. Marsh and C. G. Frost, *Chem. Commun.*, 2015, **51**, 561–564.

19 L. Zhang, T. Hou, H. Li and F. Li, *Analyst*, 2015, **140**, 4030–4036.

20 H. Zhang, C. Xu, J. Liu, X. Li, L. Guo and X. Li, *Chem. Commun.*, 2015, **51**, 7031–7034.

21 *Thermo Scientific Pierce Assay Development Technical Handbook*, Pierce Biotechnology, Rockford, IL, USA, 2011, pp. 4–5.

22 A. G. Kolhatkar, C. Dannongoda, K. Kourentzi, A. C. Jamison, I. Nekrashevich, A. Kar, E. Cacao, U. Strych, I. Rusakova, K. S. Martirosyan, D. Litvinov, T. R. Lee and R. C. Willson, *Int. J. Mol. Sci.*, 2015, **16**, 7535–7550.

23 L. F. Cao, D. Xie, M. X. Guo, H. S. Park and T. Fujita, *Trans. Nonferrous Met. Soc. China*, 2007, **17**, 1451–1455; N. Gunduz Akdogan, W. Li and G. C. Hadjipanayis, *J. Nanopart. Res.*, 2014, **16**, 1–7; M. Hogan, M. Mohamed, Z.-W. Tao, L. Gutierrez and R. Birla, *Artif. Organs*, 2015, **39**, 165–171.

24 Y. Lv, H. Wang, X. Wang and J. Bai, *J. Cryst. Growth*, 2009, **311**, 3445–3450.

25 H. Deng, X. Li, Q. Peng, X. Wang, J. Chen and Y. Li, *Angew. Chem., Int. Ed.*, 2005, **44**, 2782–2785.

26 J. E. Coleman, *Annu. Rev. Biophys. Biomol. Struct.*, 1992, **21**, 441–483; K. M. Holtz and E. R. Kantrowitz, *FEBS Lett.*, 1999, **462**, 7–11; B. Stec, K. M. Holtz and E. R. Kantrowitz, *J. Mol. Biol.*, 2000, **299**, 1303–1311.

27 A. Preechaworapun, Z. Dai, Y. Xiang, O. Chailapakul and J. Wang, *Talanta*, 2008, **76**, 424–431.

28 M. Widdrat, M. Kumari, E. Tompa, M. Posfai, A. M. Hirt and D. Faivre, *ChemPlusChem*, 2014, **79**, 1225–1233.

29 L. F. Atyaksheva, O. M. Poltorak, E. S. Chukhrai and S. A. Fedosov, *Russ. J. Phys. Chem.*, 2006, **80**, 630–633.

30 B. S. Winkler, S. M. Orselli and T. S. Rex, *Free Radical Biol. Med.*, 1994, **17**, 333–349.

31 B. S. Winkler, *Biochim. Biophys. Acta, Gen. Subj.*, 1987, **925**, 258–264.

32 A. G. Kolhatkar, I. Nekrashevich, D. Litvinov, R. C. Willson and T. R. Lee, *Chem. Mater.*, 2013, **25**, 1092–1097; R. Wirix-Speetjens, G. Reekmans, R. De Palma, C. Liu, W. Laureyn and G. Borghs, *Sens. Actuators, B*, 2007, **128**, 1–4.

33 D. Litvinov and R. Willson, Nanomagnetic Detector Array for Biomolecular Recognition, *U.S. Patent*, 8456157B2, 2013.

34 A. Cousins, G. L. Balalis, S. K. Thompson, D. Forero Morales, A. Mohtar, A. B. Wedding and B. Thierry, *Sci. Rep.*, 2015, **5**, 10842.